

Synaptic Activation of Glutamate Transporters in Hippocampal Astrocytes

Dwight E. Bergles* and Craig E. Jahr
Vollum Institute, L474
Oregon Health Sciences University
3181 SW Sam Jackson Park Road
Portland, Oregon 97201-5471

Summary

Glutamate transporters in the CNS are expressed in neurons and glia and mediate high affinity, electrogenic uptake of extracellular glutamate. Although glia have the highest capacity for glutamate uptake, the amount of glutamate that reaches glial membranes following release and the rate that glial transporters bind and sequester transmitter is not known. We find that stimulation of Schaffer collateral/commissural fibers in hippocampal slices evokes glutamate transporter currents in CA1 astrocytes that activate rapidly, indicating that a significant amount of transmitter escapes the synaptic cleft shortly after release. Transporter currents in outside-out patches from astrocytes have faster kinetics than synaptically elicited currents, suggesting that the glutamate concentration attained at astrocytic membranes is lower but remains elevated for longer than in the synaptic cleft.

Introduction

Glutamate transporters expressed in neurons and glia provide the major pathway for the uptake of glutamate released from excitatory terminals. By coupling the translocation of glutamate to the electrochemical gradients for Na^+ , K^+ , and H^+ , transporters are capable of lowering extracellular glutamate to submicromolar levels at equilibrium (Zerangue and Kavanaugh, 1996). However, extracellular glutamate concentrations are dynamic and may range from submicromolar to several millimolar in the synaptic cleft following release. The role of transporters in shaping the glutamate concentration in the synaptic cleft is controversial, in part, because the turnover rate of transporters is slow (Wadiche et al., 1995a) and because theoretical predictions suggest that the glutamate concentration can fall rapidly in the synaptic cleft by passive diffusion alone (Eccles and Jaeger, 1958). Nevertheless, competitive antagonists of glutamate transporters have been shown to slow the decay of excitatory postsynaptic currents (EPSCs) at both parallel fiber and climbing fiber synapses onto Purkinje cells (Barbour et al., 1994; Takahashi et al., 1996) and at calyceal synapses in the nucleus magnocellularis (Otis et al., 1996), suggesting that the duration of the glutamate transient in the cleft is normally curtailed by transporters. Since glutamate transporters require 50–100 ms to complete a cycle (Wadiche et al., 1995a), it has been suggested that the glutamate concentration in the vicinity of postsynaptic receptors may fall rapidly through

binding to a large number of transporters (Tong and Jahr, 1994). In support of this model, transporters have been shown to participate in clearance of the cleft on a submillisecond time scale at synapses in hippocampal cultures (Tong and Jahr, 1994; Diamond and Jahr, 1997). However, transporter antagonists do not alter the kinetics of EPSCs at Schaffer collateral synapses in hippocampal slices (Hestrin et al., 1990; Isaacson and Nicoll, 1993; Sarantis et al., 1993), suggesting that the degree to which transporters shape the transient of glutamate seen by postsynaptic receptors may depend on synapse geometry, transporter density, and other factors that vary among synapses. A caveat to these negative results is that antagonists that are themselves transported will attain greatly diminished concentrations within the slice (Sarantis et al., 1993).

The majority of synapses in the CNS are closely associated with glial processes (Palay and Chan-Palay, 1974; Spacek, 1985; Kosaka and Hama, 1986; Sorra and Harris, 1993), which increase the diffusional distance between synapses that are often less than a micrometer apart. Glial cells express two of the five glutamate transporters that have been cloned, termed GLAST and GLT-1 (rodent analogs of the human transporters EAAT1 and EAAT2, respectively) (Rothstein et al., 1994; Lehre et al., 1995), and considerable evidence suggests that these two glial transporters are responsible for the majority of glutamate uptake in the CNS. Glial profiles predominate in autoradiographs of CNS tissue incubated with L-[^3H]glutamate (McLennan, 1976; de Barry et al., 1982; Wilkin et al., 1982), and when the expression of either GLAST or GLT-1 is reduced (Rothstein et al., 1996) or eliminated (Tanaka et al., 1997), animals have elevated glutamate in the cerebrospinal fluid, an increased susceptibility to ischemic insults, and slowed clearance of glutamate at some synapses. However, it is not known how much glutamate escapes the synaptic cleft and reaches glial membranes or how long it remains elevated in the extrasynaptic space following release, factors that may be important for determining the extent to which presynaptic receptors located outside of the cleft are activated (Baude et al., 1993; Scanziani et al., 1997) and the ability of transmitter to “spill over” onto postsynaptic receptors at adjacent synapses (Kullmann et al., 1996; Silver et al., 1996; Asztely et al., 1997).

Glutamate uptake by high affinity transporters is electrogenic, a consequence of the translocation of net positive charge during each transport cycle, making it possible to monitor transport electrophysiologically (Brew and Attwell, 1987; Schwartz and Tachibana, 1990; Wyllie et al., 1991). Synaptic activation of glutamate transporter currents in glial cells has been demonstrated in culture (Mennerick and Zorumski, 1994; Linden, 1997) and recently in cerebellar slices (Clark and Barbour, 1997). The rapid onset of these currents suggests that glutamate reaches glial transporters very soon after exocytosis; however, uncertainty about the intrinsic kinetics of the transporters has prevented estimation of the glutamate profile at these extrasynaptic sites. We report here that stimulation of Schaffer collateral fibers in hippocampal

*To whom correspondence should be addressed.

slices elicits glutamate transporter currents in stratum radiatum astrocytes of area CA1. Comparison of the kinetics of synaptically activated transporter currents with those elicited in outside-out patches from astrocytes suggests that the glutamate reaches astrocytic membranes at a concentration substantially lower than the 1–3 mM thought to occur in the cleft (Clements et al., 1992; Diamond and Jahr, 1997) and remains elevated in the extracellular space for many milliseconds following release.

Results

Identification of Astrocytes

The cell bodies of astrocytes in stratum radiatum of area CA1 were visualized using infrared light and DIC optics. These cells were identified by their small somata (diameter = $\sim 10 \mu\text{m}$), low input resistances ($11.1 \pm 6.4 \text{ M}\Omega$; $n = 14$), high resting potentials ($-93.2 \pm 2.0 \text{ mV}$; $n = 14$), and passive membrane properties. When astrocytes were filled with the fluorescent dye Cy5-EDA and imaged using a confocal microscope, numerous highly branched processes could be seen extending from the soma (Figure 1A), demonstrating the complex morphology of these nonneuronal cells. Multiple cells often became labeled when a single astrocyte was loaded with the dye, demonstrating that astrocytes in slices from postnatal day 14 (P14) animals exhibit gap junctional coupling (Yamamoto et al., 1992; Koneintzko and Muller, 1994). Multiexponential fits to the passive rise and decay of the membrane potential to current pulses yielded time constants of: $\tau_{\text{fast}} = 0.20 \pm 0.07 \text{ ms}$ ($52\% \pm 7\%$), $\tau_{\text{slow}} = 1.46 \pm 0.24 \text{ ms}$ ($n = 10$) (see Figure 1B). These morphological and electrophysiological traits are characteristic of hippocampal astrocytes (Schwartzkroin and Prince, 1979; Kosaka and Hama, 1986; Koneintzko and Muller, 1994). Occasionally, members of a second class of glial cells were encountered; these cells had higher input resistances ($>500 \text{ M}\Omega$), prominent voltage-dependent K^+ currents, and did not respond to afferent stimulation (see below). These cells have been previously characterized as a class of GFAP-negative glial cells, termed "complex" cells (Steinhauser et al., 1994), and were not studied further.

Characterization of Evoked Responses in Astrocytes

Stimulation of the Schaffer collateral and commissural axons that form synaptic contacts with the dendrites of CA1 pyramidal neurons in this region elicited a current with a complex waveform in astrocytes voltage clamped at their resting potential. This current consisted of a transient outward component followed by an inward component that decayed over several seconds (Figure 1C1). Given the low resistance of the astrocyte membrane, the early components of this current may result from detection of the extracellular field potential generated by receptors on pyramidal cell membranes. The slow decay of the inward current follows the time course of potassium redistribution in the extracellular space, as measured with potassium-sensitive microelectrodes (Aitken and Somjen, 1986), suggesting that astrocytes

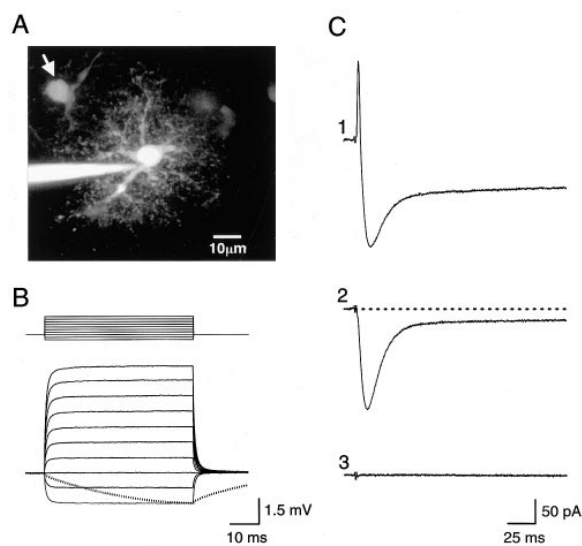


Figure 1. Stimulation of Schaffer Collateral/Commissural Fibers Elicits an Inward Current in CA1 Astrocytes

(A) Fluorescent image of an astrocyte located in stratum radiatum filled with the dye Cy5-EDA (1.5 mM), which was dissolved in the patch solution (K methanesulfonate). Numerous highly branched processes extend from the soma, and spread of the dye to adjacent astrocytes was often observed (arrow). Image is a composite of eight optical sections (step size = $10 \mu\text{m}$).

(B) Response of a CA1 astrocyte to 50 ms steps of current (-200 to 700 pA) from the resting potential ($V_m = -89 \text{ mV}$), demonstrating the low input resistance ($8.6 \text{ M}\Omega$) and fast membrane time constant ($\tau_{\text{fast}} = 0.29 \text{ ms}$, 56% ; $\tau_{\text{slow}} = 1.38 \text{ ms}$) characteristic of these cells. Broken line is the response of a CA1 pyramidal neuron to a -200 pA step, scaled to the glial response. Note the slower charging of the pyramidal cell membrane. The duration and relative amplitude of the steps is represented by the protocol displayed above the sweeps.

(C) Stimulation of afferents located in stratum radiatum elicits a current that has a complex waveform in a CA1 astrocyte voltage clamped at its resting potential ($V_m = -93 \text{ mV}$) (C1). An inward current persists in the presence of ionotropic glutamate ($10 \mu\text{M}$ NBQX, $10 \mu\text{M}$ D-CPP) and GABA_A receptor antagonists ($5 \mu\text{M}$ gabazine and $100 \mu\text{M}$ picrotoxin) (C2). When the cell was removed from the tip of the electrode, no field response was detected, confirming the block of ionotropic receptors (C3). Sweeps are averages of ten sequential responses. Stimulation = $100 \mu\text{A}$, $100 \mu\text{s}$.

detect activity-dependent changes in extracellular potassium by their high resting membrane conductance to potassium. When the slice was bathed in antagonists of ionotropic glutamate receptors, 2,3-dihydroxy-6-nitro-7-sulfamoyl-benzo(F)quinoxaline (NBQX) and R(-)-3-(2-carboxypiperazin-4-yl)-propyl-1-phosphonic acid (D-CPP), and GABA_A receptors, SR-95531 (gabazine) and picrotoxin, to block postsynaptic current flow, an inward current persisted in astrocytes in response to stimulation (Figure 1C2). This remaining inward current had a rapid onset, rose to a peak in $3.7 \pm 0.6 \text{ ms}$ (20% – 80%), and had a half decay time of $17.8 \pm 3.1 \text{ ms}$ ($n = 25$). There was also a slow phase of the decay, which was $11\% \pm 5\%$ ($n = 25$) of the peak amplitude, that required several seconds to return to baseline. When the astrocyte was removed from the tip of the electrode with positive pressure, no field response was recorded with stimulation (Figure 1C3), confirming that postsynaptic receptors were blocked.

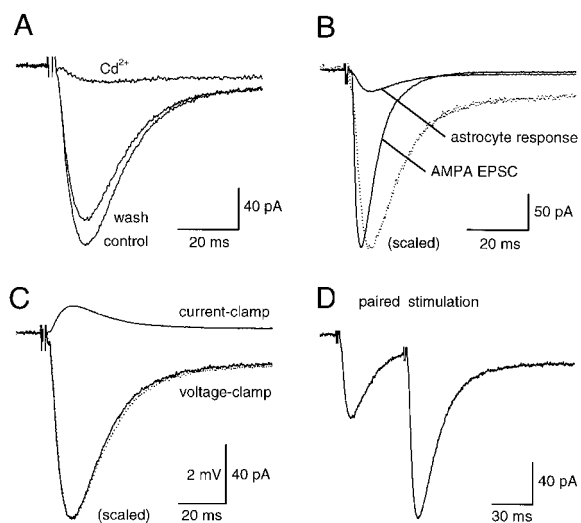


Figure 2. Characterization of Evoked Responses in Astrocytes
(A) Bath application of CdCl₂ (30 μM) inhibited the evoked inward current in stratum radiatum astrocytes, indicating the synaptic origin of these currents.
(B) Comparison of the time course of the current elicited in an astrocyte and an AMPA EPSC recorded in a CA1 pyramidal neuron in response to a stimulus of the same intensity (80 μA, 100 μs). The glial response begins at about the same time as the EPSC but rises and decays more slowly. The astrocyte was located in stratum radiatum the same distance from the stimulating electrode as the pyramidal neuron.
(C) Comparison of evoked responses in an astrocyte recorded in either current-clamp or voltage-clamp mode (V_m = -96 mV). The broken line represents the current-clamp response scaled to the voltage-clamped response.
(D) The evoked response from astrocytes exhibits paired-pulse facilitation similar to AMPA receptor-dependent EPSCs in pyramidal neurons. Interstimulus interval = 50 ms.

The glial response was synaptic in origin since inhibition of presynaptic Ca²⁺ channels through bath application of CdCl₂ (30 μM) inhibited the evoked current by 91% ± 1% (n = 9; Figure 2A). Cd²⁺ also inhibited the slowly decaying phase of the inward current by 53% ± 14% (n = 9), suggesting that a component of the astrocyte response is independent of Ca²⁺-dependent transmitter release. However, no response was elicited through antidromic stimulation of CA1 pyramidal neurons (n = 4), and the response to afferent stimulation was completely blocked by TTX (n = 3), suggesting that the current remaining in Cd²⁺ may reflect K⁺ accumulation in the extracellular space during the firing of presynaptic afferents and not direct depolarization of the glial network. The inward current elicited in astrocytes with afferent stimulation (in the presence of ionotropic glutamate and GABA_A receptor antagonists) is similar to the currents recorded from glial cells in microisland cultures in response to neuronal stimulation (Mennerick and Zorumski, 1994); the transient component of this response is due to the electrogenic uptake of glutamate by high affinity transporters (Mennerick and Zorumski, 1994). Although AMPA receptors are expressed in some hippocampal glial cells (Steinhauser et al., 1994), and glutamate released following neuronal stimulation activates these receptors in culture (Mennerick et al., 1996), it

was not possible to isolate an AMPA component of the astrocyte response in slices because of the large field current produced in the absence of NBQX.

To estimate the time course of the glial response relative to glutamate release from afferent terminals, the kinetics of the astrocyte current were compared to AMPA receptor EPSCs in CA1 pyramidal neurons. For these experiments, an AMPA receptor EPSC was first recorded from a CA1 pyramidal neuron (in D-CPP, gabazine, and picrotoxin). The slice was then bathed in NBQX, and the response to a stimulus of the same intensity was recorded from an astrocyte located in stratum radiatum at the same distance from the stimulating electrode. The glial response began without a significant delay after the onset of the AMPA EPSC, although it rose to a peak and decayed more slowly (EPSC 20%–80% rise time: 1.6 ± 0.3 ms; EPSC half decay time: 7.1 ± 1.8 ms; n = 6) (Figure 2B). Since the membrane time constant of astrocytes is much faster than the rise time of the evoked glial current, it is unlikely that electrotonic filtering can explain the kinetic differences between the glial and neuronal synaptic currents. This supposition is supported by the observation that the time course of the glial response was the same whether it was recorded in current clamp or voltage clamp (Figure 2C).

Paired stimulation of Schaffer collateral/commissural fibers results in facilitation of EPSCs in pyramidal cells, indicating that the probability of transmitter release can be increased through prior activity. Astrocyte responses also underwent facilitation when afferent fibers were stimulated at short intervals (Figure 2D), suggesting that these glial currents can also be used to monitor release probability.

Transporter Currents Elicited by Exogenous L-Glutamate

In the presence of ionotropic glutamate and GABA_A receptor antagonists (NBQX, D-CPP, gabazine, picrotoxin), brief application of L-glutamate (200 μM) to astrocytes located in stratum radiatum using a puffer pipette elicited an inward current (Figure 3A). Bath application of D,L-threo-3-hydroxyaspartate (THA; 300 μM), a broad spectrum substrate/antagonist of glutamate transporters (Balcar et al., 1977; Barbour et al., 1991), induced an inward current (-249 ± 63 pA) in these cells and inhibited the response to L-glutamate by 90% ± 4% (n = 5; Figure 3A). These data suggest that glutamate transporters are expressed in hippocampal astrocytes in situ, consistent with earlier studies demonstrating that astrocytes in brain slices accumulate L-[³H]glutamate (McLennan, 1976) and that L-glutamate elicits inward currents in astrocytes in hippocampal slices without increasing the current noise (Steinhauser et al., 1994). Dihydrokainate (DHK; 300 μM), a nontransported inhibitor selective for the glial GLT-1 transporter (Johnston et al., 1979; Arriza et al., 1994), potentiated the response to exogenous L-glutamate by 14% ± 11% (range: 3%–28%; n = 4) (Figure 3B) without producing an inward current. This potentiation may result from the high capacity of brain slices for glutamate uptake and the expression of both GLAST and GLT-1 transporters in the hippocampus at this age (Shibata et al., 1996). Inhibition

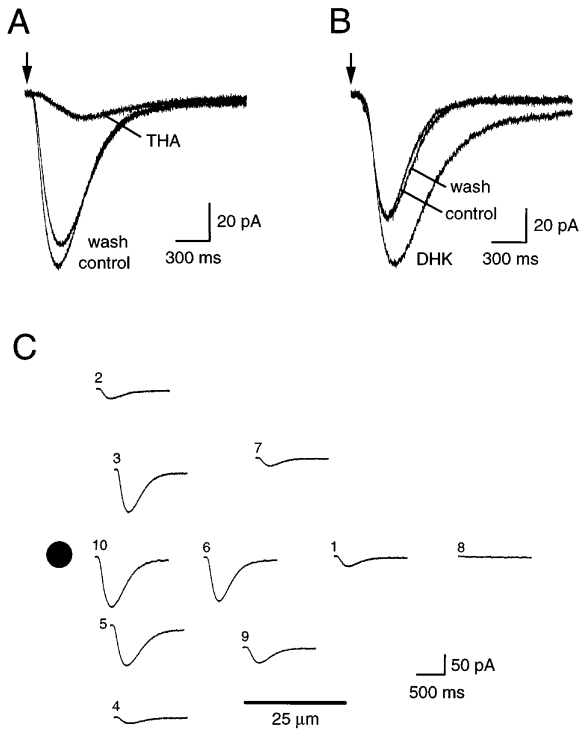


Figure 3. L-Glutamate Evoked Transporter Currents in Stratum Radiatum Astrocytes

(A) Puffer application of 200 μ M L-glutamate elicits an inward current in an astrocyte voltage clamped at its resting potential ($V_m = -88$ mV), in the presence of 10 μ M NBQX, 10 μ M D-CPP, 5 μ M gabazine, and 100 μ M picrotoxin. Bath application of the glutamate transporter substrate/antagonist THA (300 μ M) induced an inward shift in the holding current (-340 pA) and inhibited the response to exogenous L-glutamate. Arrow indicates when L-glutamate application was started (puff was 100 ms long). The response in THA has been offset by 340 pA.

(B) Bath application of DHK (300 μ M), a selective antagonist for the glial GLT-1 glutamate transporter, reversibly potentiated the response to puffer-applied L-glutamate but did not produce a change in the holding current.

(C) Response of a stratum radiatum astrocyte to the application of L-glutamate at different distances from the soma. Responses were detected only when the puffer pipette was placed within ~ 75 μ m of the cell body (indicated by the black dot). The beginning of each trace indicates the position of the puffer pipette, and the numbers correspond to the order in which the different locations were tested. Responses in (A), (B), and (C) are from the same astrocyte. K gluconate-based internal solution.

of GLT-1 transporters throughout the slice with DHK may allow more L-glutamate to reach the GLAST transporters on the astrocyte being recorded from. Both THA and DHK slowed the decay of the response, suggesting that L-glutamate remains elevated in the extracellular space for longer when uptake is inhibited.

Hippocampal astrocytes are coupled through gap junctions (Yamamoto et al., 1992; Koneintzko and Muller, 1994; see Figure 1A), raising the possibility that the current recorded from individual astrocytes in response to afferent stimulation reflects the contribution of currents produced in neighboring cells. However, L-glutamate (200 μ M) was only able to elicit transporter currents when puffs were made within approximately 75 μ m from

the soma (Figure 3C); similar results were obtained in eight other cells. These data are consistent with the high resting conductance of astrocyte membranes that should rapidly shunt an inward current, restricting its propagation to adjacent cells. These results suggest that the synaptic current recorded at the soma is locally generated and is not a distributed response of the astrocyte network.

Pharmacological Characterization of Responses Evoked through Afferent Stimulation

The pharmacological profile of the current elicited in astrocytes by stimulation of Schaffer collateral/commissural fibers in the presence of ionotropic glutamate and GABA_A receptor antagonists suggests that it is largely due to the electrogenic uptake of glutamate released from afferent terminals. This current was not inhibited by antagonists of other neurotransmitter receptors, including metabotropic glutamate receptors (MCPG, 1 mM), GABA_B receptors (CGP 55845A, 1 μ M), ATP receptors (suramin, 50 μ M), adenosine receptors (8-cyclopentyltheophylline, 4 μ M), acetylcholine receptors (hexamethonium, 200 μ M), 5-HT receptors (ondansetron, 2 μ M), glycine receptors (strychnine, 2 μ M), or β -adrenoceptors (propranolol, 1 μ M). This current was also insensitive to the GABA transporter inhibitors SKF-89976-A (25 μ M; $n = 3$) and nipecotic acid (200 μ M; $n = 4$).

In contrast to the lack of effect observed for the above antagonists, the astrocyte current was inhibited by glutamate transporter antagonists. Application of THA (300 μ M) produced an inward current (-314 ± 114 pA) and inhibited the evoked response by $37\% \pm 4\%$ ($n = 11$; Figure 4A1), while DHK (300 μ M) inhibited the current by $30\% \pm 4\%$ ($n = 8$) but did not induce an inward current (Figure 4B1). The decay of the remaining current in both cases was slowed (Figures 4A2 and 4B2), consistent with the slowing of the response to puffer-applied L-glutamate when either antagonist was present (see Figures 2A and 2B). The prolongation of the response in the presence of transporter antagonists suggests that synaptically released glutamate also remains elevated in the extracellular space longer when uptake into astrocytes is reduced. The partial inhibition of the response by DHK is consistent with the comparable levels of GLT-1 and GLAST mRNA in the hippocampus at this age (Shibata et al., 1996). The incomplete block observed with THA may indicate that a much lower concentration of this antagonist reaches the transporters because it is actively taken up while diffusing into the slice (Sarantis et al., 1993). This conclusion is supported by experiments where THA was applied together with DHK. Under these conditions, with the glial GLT-1 transporter inhibited, THA (300 μ M) induced a larger inward current (-644 ± 140 pA) and increased the inhibition of the evoked response to $72\% \pm 5\%$ ($n = 5$; Figure 4C); in two cells, only the slowly decaying phase of the response remained.

The translocation of glutamate across cell membranes by high affinity transporters is dependent on the concentration gradients for Na⁺, K⁺, and H⁺ (Brew and Attwell, 1987; Barbour et al., 1991; Zerangue and Kavanaugh, 1996), and changing these gradients can lead to reduced

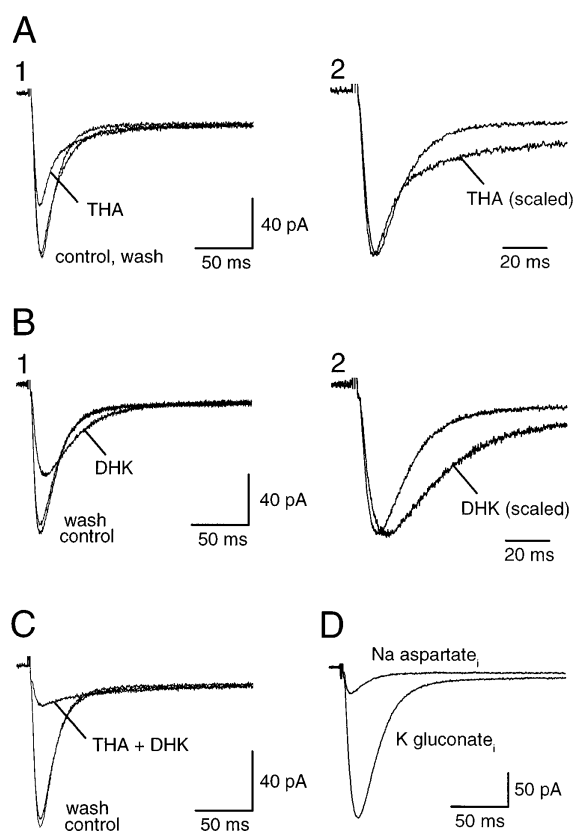


Figure 4. Pharmacological Characterization of the Astrocyte Response

(A) THA (300 μ M) induced an inward current, inhibited the response elicited through afferent stimulation, and slowed the decay of the current, visible when the response in THA is scaled to the peak of the control response (A2). The baseline of the response in THA has been offset to match that of the control response.

(B) DHK (300 μ M) inhibited the evoked response and greatly slowed the decay of the current, visible when the response in DHK is scaled to the peak of the control response (B2). No offset current was produced by DHK.

(C) When THA (300 μ M) was applied with DHK (300 μ M), it produced a larger inward shift in the holding current and a greater inhibition of the evoked response. The baseline of the response in THA plus DHK has been offset to match that of the control response.

(D) Comparison of evoked responses in two astrocytes to the same stimulus (150 μ A, 100 μ s) recorded with different internal solutions. The amplitude of glial currents recorded with a K gluconate-based internal solution was always larger than those recorded with a Na aspartate-based internal solution. Responses are from neighboring astrocytes located the same distance from the stimulating electrode.

or reversed transport (Szatkowski et al., 1990). The currents elicited in astrocytes with synaptic stimulation were also dependent on these gradients. When the composition of the standard pipette solution was changed so that K^+ was replaced with Na^+ and gluconate was replaced with D-aspartate, conditions that should reduce the number of transporters available to bind extracellular glutamate, evoked responses in astrocytes were greatly reduced in amplitude ($n = 7$; Figure 4D). For these experiments, a control response was obtained from an astrocyte with a K gluconate-based internal solution, and then the response from a nearby cell in

the same slice was recorded with a Na aspartate-based internal solution. The stimulus intensity and the approximate distance from the stimulating electrode was the same for both recordings.

Evoked Responses in Astrocytes from P7 Animals

The high resting potassium conductance in astrocytes from P14 animals prevented measurements of the current-voltage relation of the evoked response. Replacing internal K^+ with Cs^+ and adding TEA to the internal solution did not substantially reduce this conductance. However, astrocytes in slices from P7 animals had a lower resting potassium conductance and a higher input resistance (79.8 ± 37.0 M Ω , range: 53–153 M Ω ; $n = 8$), which allowed greater control of the membrane potential at electrotonically distant sites. Stimulation in the stratum radiatum region in P7 slices also elicited an inward current in CA1 astrocytes that was insensitive to ionotropic glutamate and GABA_A receptor antagonists but was blocked by THA (300 μ M; $n = 6$) (Figure 5A). The GLT-1-selective antagonist DHK inhibited these transporter currents by $41\% \pm 6\%$ (300 μ M; $n = 5$) (Figure 5B), suggesting that GLAST transporters account for more than half of the synaptic transporter current at this age. Both DHK and THA slowed the decay of the evoked current, similar to that observed in P14 animals; in THA, this slowing was visible during the onset and recovery of the block. The complete inhibition of the evoked response by THA suggests that a higher concentration of the antagonist is achieved in slices from P7 than in P14 animals, consistent with the lower glutamate uptake capacity of the hippocampus in P7 animals (Schmidt and Wolf, 1988). The higher membrane resistance of P7 astrocytes allowed us to measure the current-to-voltage relation of these synaptically evoked currents. This relation rectified inwardly, and the evoked responses did not reverse at potentials up to 60 mV (Figure 5C; $n = 4$), as expected of glutamate transporter currents under these ionic conditions (Wadiche et al., 1995b).

The rise (20%–80%) and half decay times of the synaptic transporter currents in P7 slices were 3.3 ± 0.5 ms and 25.9 ± 8.0 ms ($n = 8$), respectively. The slower decay of the synaptic transporter currents in P7 animals than those from P14 slices suggests either that the kinetics of the glutamate transporters are slower or that glutamate persists in the extracellular space for longer in P7 than in P14 animals. The latter explanation is consistent with the increase in expression levels of glutamate transporters (Shibata et al., 1996) and capacity of the hippocampus for L-glutamate uptake (Schmidt and Wolf, 1988) during the first month of development.

Glutamate Transporter Currents in Patches from Astrocytes

To estimate the concentration time course of glutamate at the astrocyte membrane following evoked release, the kinetics of glutamate transporter currents were determined. Transporter currents were elicited in outside-out patches from astrocytes by rapid applications of L-glutamate. In the presence of the ionotropic glutamate receptor antagonists, NBQX, 1-(4-aminophenyl)-4-methyl-7,8-methylenedioxy-5H-2,3-benzodiazepine hydrochloride (GYKI-52466), and D-CPP, L-glutamate (10 mM) elicited an inward current in patches when the primary anion

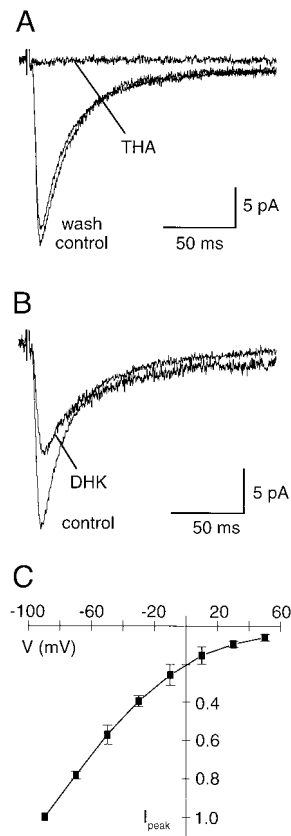


Figure 5. Evoked Responses in Astrocytes from P7 Animals
(A) THA (300 μ M) induced a steady-state inward current (-243 pA) and blocked the evoked response in astrocytes from P7 slices. The response in THA has been offset by 243 pA.
(B) DHK inhibited the evoked response and reduced the holding current by 65 pA. The response in DHK has been offset by -65 pA. Responses in (A) and (B) are from the same stratum radiatum astrocyte ($V_m = -90$ mV).
Stimulation intensity was 130 μ A. KNO_3 -based internal solution.
(C) Current-voltage relation of the synaptically activated currents from P7 astrocytes, demonstrating the prominent inward rectification and lack of reversal of the evoked responses at potentials up to 50 mV ($n = 4$).

in the pipette solution was gluconate (Figure 6A). This current was blocked by THA (300 μ M) and did not reverse at potentials up to 50 mV ($n = 5$), suggesting that it is produced by the electrogenic transport of glutamate. L-glutamate-evoked currents recorded in the absence of NBQX, GYKI, and D-CPP had the same amplitude and time course ($n = 6$), suggesting that neither AMPA nor NMDA receptors are present in the somatic membrane of hippocampal astrocytes.

The amplitude of the transporter currents in patches was small (-5.9 ± 0.9 pA; $n = 19$; 10 mM L-glutamate, $V_m = -110$ mV), which prevented accurate kinetic measurements. However, the presence of a detectable response in patches, in the absence of permeant anions (see below), suggests that these transporters are expressed at a high density in the somatic membrane of astrocytes. The density of transporters in patches was estimated by measuring the amount of charge transferred during the transient phase of the response, which

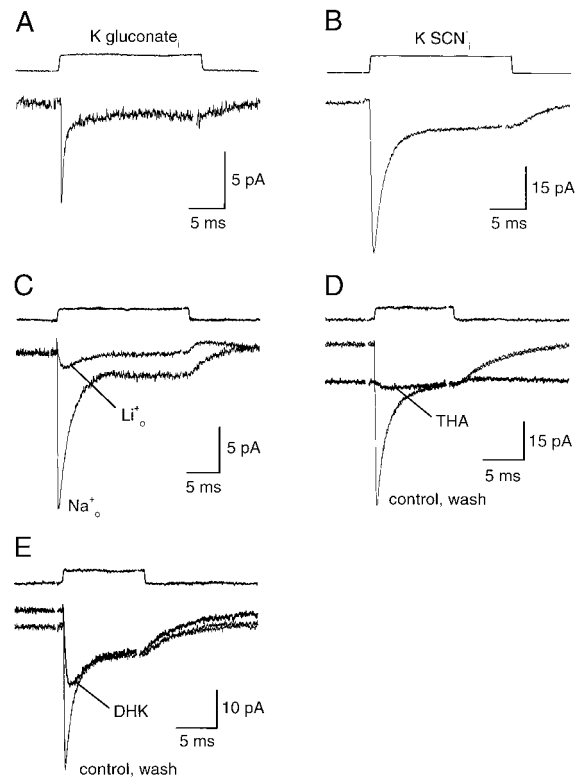


Figure 6. Transporter Currents Elicited in Outside-Out Patches from Astrocytes

(A) Rapid applications of L-glutamate (10 mM) elicited small currents with transient and steady-state components in outside-out patches in the presence of 10 μ M NBQX, 25 μ M GYKI-52466, 10 μ M D-CPP, and 5 μ M gabazine. K gluconate-based internal solution.
(B) Outside-out patch responses to L-glutamate (10 mM) were larger when the internal solution contained a permeant anion (KSCN-based internal solution) but had a similar time course.
(C) Substitution of Li⁺ for external Na⁺ inhibited patch responses to L-glutamate (10 mM). The remaining current in the Li⁺ external solution may reflect residual Na⁺ (10 mM) in the L-glutamate solution.
(D) THA (300 μ M, darker line) induced a steady-state inward current in outside-out patches and blocked responses to L-glutamate (10 mM).
(E) DHK (300 μ M, darker line) reduced an inward holding current and inhibited the response to L-glutamate.
All traces are averages of 8–15 responses recorded at -110 mV. The duration of the L-glutamate applications is indicated by the open tip response above the traces.

was 5.46 ± 8.73 fC ($n = 19$). Assuming that this charge movement reflects the early steps in the transport cycle prior to glutamate unbinding, where three Na⁺ and one H⁺ are translocated by each transporter for every molecule of glutamate transported (Zerangue and Kavanaugh, 1996), this net movement of three positive charges corresponds to an average of $18,200 \pm 29,100$ transporters/patch ($n = 19$). The membrane area of these patches was estimated according to the method of Karpen et al. (1992) by measuring the capacitance before and after pushing the pipette against a Sylgard bead on the tip of a second electrode. Subtraction of the pipette and stray capacitances using this method yielded the capacitance of the patch membrane, which

was converted to area assuming a specific membrane capacitance of $1 \mu\text{F}/\text{cm}^2$. In five patches, the area ranged from 1.3 to $18.2 \mu\text{m}^2$ ($6.64 \pm 6.9 \mu\text{m}^2$). These data suggest that glutamate transporters are present on the somatic membrane of astrocytes at a density of more than $2,500 \mu\text{m}^{-2}$.

Substitution of SCN^- for gluconate in the pipette solution greatly increased the size of the response to L-glutamate ($-55.2 \pm 8.8 \text{ pA}$; $n = 32$; 10 mM L-glutamate, $V_m = -110 \text{ mV}$) (Figure 6B), as expected from the high permeability of GLT-1, GLAST, and other glial glutamate transporters to chaotropic anions (Wadiche et al., 1995b; Eliasof and Jahr, 1996; Kavanaugh et al., 1997). These L-glutamate-evoked transporter currents were inhibited when external Na^+ was replaced with Li^+ ($n = 5$; Figure 6C), consistent with the dependence of glutamate transporters on cotransported Na^+ (Brew and Attwell, 1987; Mennerick and Zorumski, 1994). THA ($300 \mu\text{M}$) induced an inward current in these patches and inhibited the response to L-glutamate (10 mM) by $95\% \pm 3\%$ ($n = 5$; Figure 6D), similar to that observed in whole-cell recordings. DHK also inhibited the peak of the response to L-glutamate ($n = 6$), consistent with the contribution of GLT-1 to this current (Figure 6E); however, it was not possible to quantitate the amount of inhibition by DHK, because it also reduced an inward holding current. This reduction in holding current suggests that there is an uncoupled movement of SCN^- through the transporter that is blocked by DHK. This is further supported by the voltage dependence of the current blocked by DHK ($300 \mu\text{M}$), which matched the voltage dependence of the transporter conductance. Inhibition of an anion "leak" through transporters was also visible in whole-cell recordings from astrocytes in slices; bath application of DHK ($300 \mu\text{M}$) produced an outward current when cells were loaded with the permeant anion NO_3^- ($76.2 \pm 21.8 \text{ pA}$; $n = 6$; P7 astrocytes) but not gluconate, an impermeant anion (Wadiche et al., 1995b). This effect of DHK was not observed in patches from Bergmann glial cells (D. E. B. and C. E. J., unpublished data), which express primarily GLAST (Rothstein et al., 1994; Lehre et al., 1995; Shibata et al., 1996), suggesting that either there is no anion leak through the GLAST transporter or the ability of DHK (at $300 \mu\text{M}$) to inhibit the leak is selective for the GLT-1 transporter. The latter possibility is consistent with the higher affinity of DHK for GLT-1 (Arriza et al., 1994). The uncoupled movement of monovalent cations through glutamate transporters has been demonstrated in retinal Muller cells (Schwartz and Tachibana, 1990) and the cloned EAAT1 and EAAC3 transporters (Kanai et al., 1995; Kavanaugh et al., 1997); however, the substrate-independent movement of anions through native or cloned glutamate transporters has not yet been described.

The current-to-voltage relation of L-glutamate evoked currents in patches rectified inwardly, changing e-fold over 63 mV (positive to -110 mV), and did not reverse at potentials up to 50 mV ($n = 10$; Figures 7A and 7B), similar to the synaptic transporter currents recorded from astrocytes in P7 animals. Patch currents decayed to a steady-state level during L-glutamate application. The mechanism of this decay is not known but may reflect desynchronization of the transporters (Brunts et

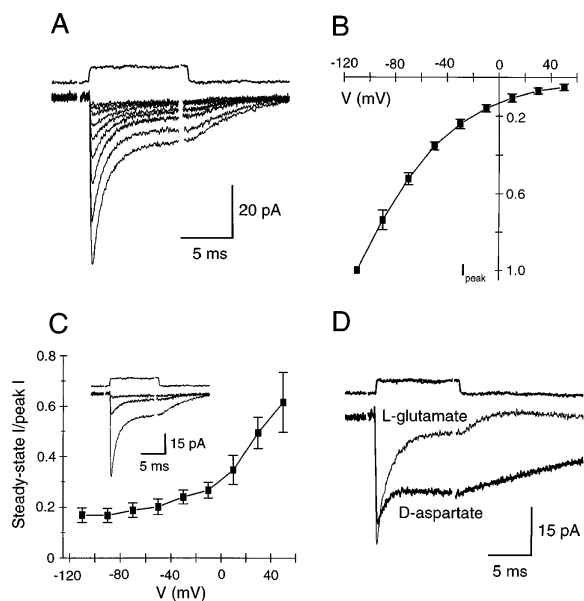


Figure 7. Voltage Dependence of Astrocyte Glutamate Transporter Currents in Patches

(A) L-glutamate (10 mM) evoked transporter currents in an outside-out patch from a CA1 astrocyte at a range of holding potentials (-110 to 50 mV). The duration of glutamate application is indicated by the open tip current above the traces.

(B) Plot of the current-to-voltage relation for ten patches, demonstrating the prominent inward rectification and lack of reversal characteristic of glutamate transporter currents. Values were normalized to responses at -110 mV .

(C) The ratio of the steady-state to peak amplitude of the response to 10 mM L-glutamate increased with depolarization. Inset shows the response at -110 mV , -30 mV , and 50 mV .

(D) The steady-state to peak ratio was greater for D-aspartate (dark trace), an agonist with a greater affinity for the transporter, than for L-glutamate. The concentration of both agonists was 10 mM .

et al., 1993) as they reach nonconducting states in the transport pathway. This conclusion is supported by the increase in the steady-state to peak ratio with depolarization (Figure 7C) and the slower kinetics and larger steady-state current observed with D-aspartate (steady-state/peak ratio: L-glutamate, 0.07 ± 0.05 ; D-aspartate, 0.52 ± 0.15 ; $n = 5$; Figure 7D), which has a higher apparent affinity and slower transport rate than L-glutamate (Arriza et al., 1994; Wadiche et al., 1995a). Paired pulses of L-glutamate were applied to patches to measure the recovery time of these transporters from the desynchronized or steady-state level. The recovery of the response to the control amplitude followed a biexponential time course: ($\tau_{\text{fast}} = 14.5 \text{ ms}$, 79% ; $\tau_{\text{slow}} = 108.5 \text{ ms}$; Figure 8A). The biexponential recovery suggests that there are at least two pathways from the conducting state to the unbound state, one of which is faster than a complete transport cycle (estimated at 70 ms for GLT-1; Wadiche et al., 1995a).

The apparent affinity of the transporters for L-glutamate and the concentration dependence of their kinetics were measured by applying a range of L-glutamate concentrations to individual patches. The EC_{50} of the steady-state current was $13 \pm 4 \mu\text{M}$ ($n = 8$; P14 astrocytes), similar to steady-state measurements of K_m for the

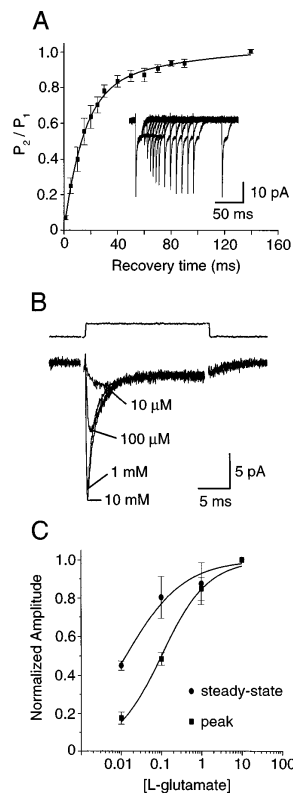


Figure 8. Paired-Pulse Recovery and Dose-Response Relation of Glutamate Responses in Patches

(A) Plot of the ratio of the peak amplitude of the second (P_2) to the first (P_1) response of patches to paired applications of L-glutamate (10 mM). The second applications were given 1–140 ms after the end of the first application ($n = 6$). Line is a biexponential fit to the data.

(B) Transporter currents evoked in an individual patch by 10 μ M, 100 μ M, 1 mM, and 10 mM L-glutamate. All responses were recorded at -110 mV.

(C) Dose-response relation of the responses of patches to a range of L-glutamate concentrations (10 μ M to 10 mM) recorded at -100 mV. The EC_{50} for the peak (100 ± 13 μ M, $n_H = 0.73$) was greater than the EC_{50} for the steady-state (13 ± 4 μ M; $n = 8$; $n_H = 0.59$). Data were fit with the logistic equation.

cloned GLT-1 and GLAST transporters (2 μ M and 13 μ M, respectively) (Pines et al., 1992; Klockner et al., 1994). The apparent affinity of the peak response was lower ($EC_{50} = 100 \pm 13$ μ M; $n = 8$). The different apparent affinities of the peak and steady-state responses suggests that there are additional long-lived, nonconducting states in the transport cycle that are reached at steady-state. The rise time (20%–80%) of these currents in patches from P14 astrocytes was 95 ± 30 μ s for 10 mM, 125 ± 26 μ s for 1 mM, 350 ± 111 μ s for 100 μ M, and 2.16 ± 0.67 ms for 10 μ M ($n = 8$; Figure 8B). The rapid kinetics of these transporter currents in patches suggests that the time course of the synaptic response is not limited by the kinetics of the transporters. The half decay time of the transporter currents in patches, either measured during L-glutamate application (1.35 ± 0.26 ms; 10 mM L-glutamate) or at the end of glutamate application (2.91 ± 0.48 ms; $n = 8$), was also faster than the half decay time of the synaptic currents (17.8 ms),

suggesting that glutamate remains elevated at glial membranes for many milliseconds following exocytosis. Transporter kinetics were also fast in patches from P7 astrocytes (20%–80% rise time = 130 ± 20 μ s; half decay time = 1.5 ± 0.24 ms; $n = 4$; 10 mM L-glutamate), suggesting that the slower decay of evoked transporter currents in P7 astrocytes than in P14 astrocytes reflects a slower clearance of glutamate from the extracellular space in the hippocampus of younger animals.

Discussion

Astrocytes in the CNS accumulate radiolabeled glutamate and aspartate (McLennan, 1976; de Barry et al., 1982; Wilkin et al., 1982), express glutamate transporters at a high density (Rothstein et al., 1994; Lehre et al., 1995), and have processes that are associated with most excitatory synapses (Spacek, 1971, 1985; Sorra and Harris, 1993). We demonstrate here that stimulation of the Schaffer collateral/commissural fibers in hippocampal slices elicits a current in astrocytes located in stratum radiatum of area CA1 that is mediated, in part, by the electrogenic uptake of glutamate. Synaptic activation of glutamate transporters in glial cells has been reported in hippocampal (Mennerick and Zorumski, 1994) and cerebellar cultures (Linden, 1997) and recently in Bergmann glial cells in cerebellar slices (Clark and Barbour, 1997). In these studies, the glial currents began with little delay after stimulation, suggesting that glutamate diffuses out of the cleft rapidly, reaching some of the glial transporters within a millisecond following release. Although rapid in onset, transporter currents recorded from hippocampal astrocytes rose to a peak more slowly than AMPA EPSCs in pyramidal neurons and decayed over tens of milliseconds. The slower time course of the synaptic transporter current may reflect the kinetics of the transporters or the duration that glutamate remains elevated at the astrocyte membrane.

Relationship between the Anion Conductance and Glutamate Transport

The currents produced in outside-out patches from astrocytes by L-glutamate revealed that glutamate transporters have rapid kinetics and are capable of binding glutamate on a submillisecond time scale. This indicates that the binding rate of these transporters for glutamate is similar to that estimated for ionotropic glutamate receptors (Jonas and Sakmann, 1992) and is consistent with the rapid buffering of synaptically released glutamate by transporters (Tong and Jahr, 1994; Diamond and Jahr, 1997). We exploited the high permeability of these transporters to chaotropic anions (Wadiche et al., 1995b; Eliasof and Jahr, 1996; Kavanaugh et al., 1997) to increase the size of transporter currents in patches. The relationship of the associated anion conductance to the stoichiometrically coupled movement of cations during glutamate translocation is not known. Preliminary analysis indicates that the small transient inward currents in patches recorded without permeant anions were faster than those recorded in the presence of permeant anions (compare Figures 7A and 7B). This observation suggests either that positive charge(s) bind within the

membrane field after glutamate binds or that translocation of positive charge across the field occurs very rapidly after glutamate binds. In either case, these events would have to precede or coincide with the rapid gating of the anion conductance. Mutant GLT-1 transporters lacking K^+ -stimulated transport are still capable of Na-dependent exchange of L-glutamate and exhibit an associated anion conductance indistinguishable from wild-type GLT-1 (Kavanaugh et al., 1997), further suggesting that the gating of the anion current is associated with the early steps in the transport cycle involving the binding and translocation of glutamate. Regardless of the ordering of these events, transporter currents in patches were much faster than those elicited synaptically, except those evoked by the lowest glutamate concentration (10 μ M), and the time course of the synaptic currents was not affected by the presence of permeant anions, suggesting that factors other than the kinetics of the transporters determine the time course of the synaptic response.

Mechanisms of the Time Course of Evoked Glutamate Transporter Currents

The slower decay of the synaptic transporter currents compared to those elicited in patches is likely to be due to a combination of mechanisms, including release asynchrony, electrotonic filtering, and diffusion of transmitter to distant sites on astrocyte membranes. The relative contribution of these factors to the time course of the synaptic currents is not known. Asynchrony in evoked responses has been reported at excitatory synapses in hippocampal cultures (Diamond and Jahr, 1995) and in slices of the anteroventral cochlear nucleus (Isaacson and Walmsley, 1995). Although its significance in hippocampal slices has not been assessed, the release rate in hippocampal cultures, determined by deconvolving the average miniature EPSC from the average EPSC, decayed with a time constant of 3.9 ms (Diamond and Jahr, 1995). If similar asynchrony occurs in slices, it could not account entirely for the slow time course of the transporter currents in astrocytes. In addition, comparison of AMPA EPSCs in pyramidal cells with synaptic transporter currents in astrocytes in the same slice (see Figure 2B), where release asynchrony is presumably the same, revealed that the transporter currents were slower than EPSCs.

The degree of slowing of the synaptic response due to electrotonic filtering is difficult to estimate. The very low input resistance of astrocytes will have two effects. First, it results in a fast membrane time constant ($\tau_{\text{slow}} \approx 1.5$ ms; Figure 1B), and second, it undoubtedly limits the signal recorded with the somatic electrode to conductance changes occurring close to the soma, underestimating the number of transporters activated by synaptic release. Both consequences of a low membrane resistance will diminish the degree of slowing of the current by electrotonic filtering (Spruston et al., 1993; Zhang and Trussell, 1994). However, the distribution of the potassium conductance is nonuniform (Newman, 1986), and the internal resistance of the thin glial processes that are intimately associated with synapses (Kosaka and Hama, 1986) is not known. These parameters

will have to be measured to predict accurately the effect of passive properties on distally generated responses recorded at the soma.

If glutamate diffuses some distance from release sites and the distribution of transporters on astrocyte membranes is not restricted to those regions nearest to synaptic clefts, then activation of some transporters will be delayed, slowing the kinetics of the transporter current. A lower concentration of glutamate would presumably reach these distant transporters, which would also slow the activation of the transporters, because binding is concentration-dependent. In P7 animals, extracellular glutamate appears to remain elevated longer after release than in P14 animals, since the synaptic transporter current decays more slowly in P7 astrocytes, and the kinetics of transporter currents in patches from these cells are also fast. This developmental difference may be due to the increased expression of transporters with age (Shibata et al., 1996) and the resulting higher capacity of the hippocampus for glutamate uptake in older animals (Schmidt and Wolf, 1988).

Implications for Activation of Glutamate Receptors at Distant Sites

We propose that in the CA1 region of the hippocampus, some of the glutamate released from excitatory terminals escapes the synaptic cleft within a millisecond of exocytosis and remains elevated at glial membranes for over 10 ms. This hypothesis is based on the comparison of transporter kinetics activated synaptically with those in patches, and it assumes that the properties of transporters are not greatly altered by patch excision. An elevation of glutamate lasting this long implies that glutamate may diffuse many micrometers from release sites. Because individual synapses in this region of the hippocampus are often less than 1 μ m apart (Sorra and Harris, 1993), glutamate released at one synapse will inevitably reach receptors at neighboring sites, unless transporters are preferentially expressed in membranes surrounding synapses to provide a barrier to the diffusion of glutamate into the cleft. If synapses are not protected from this "spill over" of glutamate, high affinity receptors such as NMDA and metabotropic glutamate receptors could be activated at synapses where release has not occurred (Kullmann et al., 1996; Asztely et al., 1997; Scanziani et al., 1997). In addition, since AMPA receptors are desensitized by low concentrations of glutamate (Kiskin et al., 1986; Trussell and Fischbach, 1989), evoked responses could be depressed by both presynaptic and postsynaptic mechanisms. The data presented here indicating that glutamate remains elevated at glial membranes for many milliseconds suggests an important role for astrocyte transporters in regulating the extent to which receptors at neighboring synapses in the hippocampus are activated.

Experimental Procedures

Hippocampal slices were prepared from 7- to 16-day-old rats using standard techniques (Sakmann and Stuart, 1995). Hippocampi were dissected free of each hemisphere, immobilized in agar, and cut into 400 μ m thick slices with a vibratome (Technical Products International) in ice cold artificial cerebral spinal fluid (ACSF) containing (in mM): 119 NaCl, 2.5 KCl, 2.5 CaCl_2 , 1.3 MgCl_2 , 1 NaH_2PO_4 , 26.2

NaHCO₃, and 11 glucose, saturated with 95% O₂/5% CO₂. Slices were stored submerged in ACSF warmed to 34°C for 30 min and at room temperature thereafter. All experiments were performed at room temperature.

Astrocyte somata located in stratum radiatum were visualized with a 40× water immersion objective (Zeiss) using a microscope equipped with IR/DIC optics (Zeiss Axioskop) and a CCD camera (Hamamatsu). Whole-cell and patch pipettes were fabricated from Corning #0010 glass (World Precision Instruments, Sarasota, FL) and had resistances of 1.5–3 MΩ. The pipette solution contained (in mM): 130 mM K⁺A⁻, 20 HEPES, 10 EGTA, 1 MgCl₂ (pH 7.2). A⁻ denotes gluconate, methanesulfonate, NO₃⁻, or SCN⁻, as stated in the text. Holding potentials have been corrected for the different junction potentials between these solutions and the ACSF.

Synaptic transport currents were evoked by passing constant-current pulses (10–140 μA, 100 μs) through a bipolar stainless steel stimulating electrode (tip separation = 200 μm) placed in stratum radiatum >150 μm away from the cell. In P7 animals, it was necessary to place the stimulating electrode within 100 μm of the cell to elicit a response. Synaptic currents were recorded using an Axopatch 200A amplifier (Axon Instruments, Foster City, CA), filtered at 1–2 kHz and digitized at 10 kHz. Current-clamp recordings of passive membrane properties were made with an Axoclamp 2A amplifier. Access resistance was monitored continuously throughout the experiments and was typically less than 10 MΩ; experiments where it changed more than 20% were excluded from the data. In experiments where picrotoxin and gabazine were used, a cut was made between CA3 and CA1 to reduce the propagation of epileptiform bursts to CA1. Slices were continuously superfused with ACSF at a rate of 2–4 ml/min, and solution changes were made using three-way stopcocks. The adenosine antagonist CPT (1–4 μM) was often added to the control ACSF to increase the amplitude of evoked responses by reducing presynaptic inhibition by ambient adenosine. This antagonist did not affect the time course of the evoked responses. Sweeps are averages of 5–20 responses, and stimulation artifacts have been truncated. All whole-cell recordings were made with a K gluconate–based internal solution unless otherwise noted.

Exogenous L-glutamate was applied to cells in slices using brief (20–50 ms) pulses of pressure (10–20 psi) applied to the back of a patch electrode using a Picospritzer (General Valve Corp., Fairfield, NJ). Puffer pipettes were filled with 200 μM L-glutamate dissolved in ACSF containing antagonists. The location of the puffer and recording pipettes was recorded on videotape, and relative distances were measured off-line.

Outside-out patches were excised from the cell bodies of astrocytes in slices following rupture of the membrane beneath the pipette. Rapid solution changes at the tip of the pipette were made using a piezoelectric bimorph to move 4-barrel electrodes as described previously (Tong and Jahr, 1994). Patch recordings were made in an external solution containing (in mM): 135 NaCl, 5.4 KCl, 5 HEPES, 1.8 CaCl₂, 1.3 MgCl₂ (pH 7.2). Adjusting this extracellular solution to match the ion concentrations used for whole-cell recordings did not alter the amplitude or kinetics of the transporter currents. The 20%–80% exchange time of the system was <200 μs as measured from the “open tip” response to the junction current arising from the movement between the solutions listed. A range of L-glutamate concentrations was applied to individual patches by connecting a miniature manifold (Warner Instruments, Hamden, CT) to one side of a theta pipette, which was attached to a bimorph. Patch currents were filtered at 5 kHz and digitized at 30–50 kHz. Artifacts arising from applying voltage steps to the bimorph have been blanked. Data are expressed as mean ± SD. All patch recordings were made with a KSCN-based internal solution unless otherwise noted.

The drugs used and their sources were: NBQX (gift from Novo Nordisk); D-CPP, CPT, nipecotic acid, picrotoxin, and SR-95531 (Research Biochemicals International); MCPG (Tocris); SKF-89976-A (gift from SmithKline Beecham), CGP 55845A (gift from Ciba-Geigy); THA, DHK, strychnine, propranolol, and hexamethonium (Sigma); ondansetron (gift from J. T. Williams); suramin (Calbiochem); Cy5-EDA (Biological Detection Systems).

Acknowledgments

We thank J. S. Diamond, J. A. Dzubay, M. P. Kavanaugh, T. S. Otis, and J. I. Wadiche for helpful discussions and comments on the manuscript and J. T. Williams for help with confocal microscopy. This work was supported by the National Institutes of Health.

Received September 22, 1997; revised October 24, 1997.

References

- Aitken, P.G., and Somjen, G.G. (1986). The sources of extracellular potassium accumulation in the CA1 region of hippocampal slices. *Brain Res.* 369, 163–167.
- Arriza, J.L., Fairman, W.A., Wadiche, J.I., Murdoch, G.H., Kavanaugh, M.P., and Amara, S.G. (1994). Functional comparisons of three glutamate transporter subtypes cloned from human motor cortex. *J. Neurosci.* 14, 5559–5569.
- Asztely, F., Erdemli, G., and Kullmann, D.M. (1997). Extrasynaptic glutamate spillover in the hippocampus: dependence on temperature and the role of active glutamate uptake. *Neuron* 18, 281–293.
- Balcar, V.J., Johnston, G.A.R., and Twitichin, B. (1977). Stereo-specificity of the inhibition of L-glutamate and L-aspartate high affinity uptake in rat brain slices by threo-3-hydroxyaspartate. *J. Neurochem.* 28, 1145–1146.
- Barbour, B., Brew, H., and Attwell, D. (1991). Electrogenic uptake of glutamate and aspartate into glial cells isolated from the salamander retina. *J. Physiol.* 436, 169–193.
- Barbour, B., Keller, B., Llano, I., and Marty, A. (1994). Prolonged presence of glutamate during excitatory synaptic transmission to cerebellar Purkinje cells. *Neuron* 12, 1331–1343.
- Baude, A., Nusser, Z., Roberts, J.D.B., Mulvihill, E., McIllhinney, R.A.J., and Somogyi, P. (1993). The metabotropic glutamate receptor (mGluR1α) is concentrated at perisynaptic membrane of neuronal subpopulations as detected by immunogold reaction. *Neuron* 11, 771–787.
- Brew, H., and Attwell, D. (1987). Electrogenic glutamate uptake is a major current carrier in the membrane of axolotl retinal glial cells. *Nature* 327, 707–709.
- Bruns, D., Engert, F., and Lux, H.-D. (1993). A fast activating presynaptic reuptake current during serotonergic transmission in identified neurons of *Hirudo*. *Neuron* 10, 559–572.
- Clark, B.A., and Barbour, B. (1997). Currents evoked in Bergmann glial cells by parallel fibre stimulation in rat cerebellar slices. *J. Physiol.* 502, 335–350.
- Clements, J.D., Lester, R.A., Tong, G., Jahr, C.E., and Westbrook, G.L. (1992). The time course of glutamate in the synaptic cleft. *Science* 258, 1498–1501.
- de Barry, J., Langley, O.K., Vincendon, G., and Gombos, G. (1982). L-glutamate and L-glutamine uptake in adult rat cerebellum: an autoradiographic study. *Neuroscience* 7, 1289–1297.
- Diamond, J.S., and Jahr, C.E. (1995). Asynchronous release of synaptic vesicles determines the time course of the AMPA receptor-mediated EPSC. *Neuron* 15, 1097–1107.
- Diamond, J.S., and Jahr, C.E. (1997). Transporters buffer synaptically released glutamate on a millisecond time scale. *J. Neurosci.* 17, 4672–4687.
- Eccles, J.C., and Jaeger, J.C. (1958). The relationship between the mode of operation and the dimensions of the junctional regions at synapses and motor end-organs. *Proc. R. Soc. Lond. [Biol.]* 148, 38–56.
- Eliasof, S., and Jahr, C.E. (1996). Retinal glial cell glutamate transporter is coupled to an anionic conductance. *Proc. Natl. Acad. Sci. USA* 93, 4153–4158.
- Hestrin, S., Sah, P., and Nicoll, R.A. (1990). Mechanisms generating the time course of dual component excitatory synaptic currents recorded in hippocampal slices. *Neuron* 5, 247–253.
- Isaacson, J.S., and Nicoll, R.A. (1993). The uptake inhibitor L-trans-PDC enhances responses to glutamate but fails to alter the kinetics

- of excitatory synaptic currents in the hippocampus. *J. Neurophysiol.* **70**, 2187–2191.
- Isaacson, J.S., and Walmsley, B. (1995). Counting quanta: direct measurements of transmitter release at a central synapse. *Neuron* **15**, 1–20.
- Johnston, G.A.R., Kennedy, S.M.E., and Twitchin, B. (1979). Action of the neurotoxin kainic acid on high affinity uptake of L-glutamic acid in rat brain slices. *J. Neurochem.* **32**, 121–127.
- Jonas, P., and Sakmann, B. (1992). Glutamate receptor channels in isolated patches from CA1 and CA3 pyramidal cells of rat hippocampal slices. *J. Physiol.* **455**, 143–171.
- Kanai, Y., Nussberger, S., Romero, M.F., Boron, W.F., Hebert, S.C., and Hediger, M.A. (1995). Electrogenic properties of the epithelial and neuronal high affinity glutamate transporter. *J. Biol. Chem.* **270**, 16561–16568.
- Karpen, J.W., Loney, D.A., and Baylor, D.A. (1992). Cyclic GMP-activated channels of salamander retinal rods: spatial distribution and variation in responsiveness. *J. Physiol.* **448**, 257–274.
- Kavanaugh, M.P., Bendahan, A., Zerangue, N., Zhang, Y., and Kanner, B.I. (1997). Mutation of an amino acid residue influencing potassium coupling in the glutamate transporter GLT-1 induces obligate exchange. *J. Biol. Chem.* **272**, 1703–1708.
- Kislin, N.I., Krishtal, O.A., and Tsyndrenko, A.Y. (1986). Excitatory amino acid receptors in hippocampal neurons: kainate fails to desensitize them. *Neurosci. Lett.* **63**, 225–230.
- Klockner, U., Storck, T., Conradt, M., and Stoffel, W. (1994). Functional properties and substrate specificity of the cloned L-glutamate/L-aspartate transporter GLAST-1 from rat brain expressed in *Xenopus* oocytes. *J. Neurosci.* **14**, 5759–5765.
- Koneintzko, U., and Muller, C.M. (1994). Astrocyte dye coupling in rat hippocampus: topography, developmental onset and modulation by protein kinase C. *Hippocampus* **4**, 297–306.
- Kosaka, T., and Hama, K. (1986). Three-dimensional structure of astrocytes in the rat dentate gyrus. *J. Comp. Neurol.* **249**, 242–260.
- Kullmann, D.M., Erdemli, G., and Asztely, F. (1996). LTP of AMPA and NMDA receptor-mediated signals: evidence for presynaptic expression and extrasynaptic glutamate spill-over. *Neuron* **17**, 461–474.
- Lehre, K.P., Levy, L.M., Ottersen, O.P., Storm-Mathisen, J., Danbolt, N.C. (1995). Differential expression of two glial glutamate transporters in the rat brain: quantitative and immunocytochemical observations. *J. Neurosci.* **15**, 1835–1853.
- Linden, D.J. (1997). Long-term potentiation of glial synaptic currents in cerebellar culture. *Neuron* **18**, 983–994.
- McLennan, H. (1976). The autoradiographic localization of L-[³H]glutamate in rat brain tissue. *Brain Res.* **115**, 139–144.
- Mennerick, S., and Zorumski, C.F. (1994). Glial contribution to excitatory transmission in cultured hippocampal cells. *Nature* **368**, 59–62.
- Mennerick, S., Benz, A., and Zorumski, C.F. (1996). Components of glial responses to exogenous and synaptic glutamate in rat hippocampal microcultures. *J. Neurosci.* **16**, 55–64.
- Newman, E.A. (1986). High potassium conductance in astrocyte endfeet. *Nature* **233**, 453–454.
- Otis, T., Wu, Y.-C., and Trussell, L.O. (1996). Delayed clearance of transmitter and the role of glutamate transporters at synapses with multiple release sites. *J. Neurosci.* **16**, 1634–1644.
- Palay, S.L., and Chan-Palay, V. (1974). *Cerebellar Cortex, Cytology and Organization* (New York: Springer-Verlag).
- Pines, G., Danbolt, N.C., Bjoras, M., Zhang, Y., Bendahan, A., Eide, L., Koepsell, H., Storm-Mathisen, J., Seeberg, E., and Kanner, B.I. (1992). Cloning and expression of a rat brain L-glutamate transporter. *Nature* **360**, 464–467.
- Rothstein, J.D., Martin, L., Levey, A.I., Dykes-Hoberg, M., Jin, L., Wu, D., Nash, N., and Kuncl, R.W. (1994). Localization of neuronal and glial glutamate transporters. *Neuron* **13**, 713–725.
- Rothstein, J.D., Dykes-Hoberg, M., Pardo, C.A., Bristol, L.A., Jin, L., Kunc, R.W., Kanai, Y., Hediger, M.A., Wang, Y., Schielke, J.P., and Welty, D.F. (1996). Knockout of glutamate transporters reveals a major role for astroglial transport in excitotoxicity and clearance of glutamate. *Neuron* **16**, 675–686.
- Sakmann, B., and Stuart, G. (1995). Patch pipette recordings from the soma, dendrites, and axon of neurons in brain slices. In *Single Channel Recording*, B. Sakmann and E. Neher, eds. (New York, New York: Plenum Press), pp. 199–211.
- Sarantis, M., Ballerini, L., Miller, B., Silver, R.A., Edwards, M., and Attwell, D. (1993). Glutamate uptake from the synaptic cleft does not shape the decay of the non-NMDA component of the synaptic current. *Neuron* **11**, 541–549.
- Scanziani, M., Salin, P.A., Vogt, K.E., Malenka, R.C., and Nicoll, R.A. (1997). Use-dependent increases in glutamate concentration activate presynaptic metabotropic glutamate receptors. *Nature* **385**, 630–634.
- Schmidt, W., and Wolf, G. (1988). High affinity uptake of L-[³H]glutamate and D-[³H]aspartate during postnatal development of the hippocampal formation: a quantitative autoradiographic study. *Exp. Brain Res.* **70**, 50–54.
- Schwartz, E.A., and Tachibana, M. (1990). Electrophysiology of glutamate and sodium co-transport in a glial cell of the salamander retina. *J. Physiol.* **426**, 43–80.
- Schwartzkroin, P.A., and Prince, D.A. (1979). Recordings from presumed glial cells in the hippocampal slice. *Brain Res.* **161**, 533–538.
- Shibata, T., Watanabe, M., Tanaka, K., Wada, K., and Inoue, Y. (1996). Dynamic changes in expression of glutamate transporter mRNAs in developing brain. *Neuroreport* **7**, 705–709.
- Silver, R.A., Cull-Candy, S.G., and Takahashi, T. (1996). Non-NMDA glutamate receptor occupancy and open probability at a rat cerebellar synapse with single and multiple release sites. *J. Physiol.* **494**, 231–250.
- Sorra, K.E., and Harris, K.M. (1993). Occurrence and three-dimensional structure of multiple synapses between individual radiatum axons and their target pyramidal cells in hippocampal area CA1. *J. Neurosci.* **13**, 3736–3748.
- Spacek, J. (1971). Three-dimensional reconstructions of astroglia and oligodendroglia cells. *Z. Zellforsch.* **112**, 430–442.
- Spacek, J. (1985). Three-dimensional analysis of dendritic spines III. Glial sheath. *Anat. Embryol.* **171**, 245–252.
- Spruston, N., Jaffe, D.B., Williams, S.H., and Johnston, D. (1993). Voltage- and space-clamp errors associated with the measurement of electrotonically remote synaptic events. *J. Neurophysiol.* **70**, 781–802.
- Steinhauser, C., Jabs, R., and Kettenmann, H. (1994). Properties of GABA and glutamate responses in identified glial cells of the mouse hippocampal slice. *Hippocampus* **4**, 19–36.
- Szatkowski, M., Barbour, B., and Attwell, D. (1990). Non-vesicular release of glutamate from glial cells by reversed electrogenic glutamate uptake. *Nature* **348**, 443–446.
- Takahashi, M., Sarantis, M., and Attwell, D. (1996). Postsynaptic glutamate uptake in rat cerebellar Purkinje cells. *J. Physiol.* **497**, 523–530.
- Tanaka, K., Watase, K., Manabe, T., Yamada, K., Watanabe, M., Takahashi, K., Iwama, H., Nishikawa, T., Ichihara, N., Kikuchi, T., et al. (1997). Epilepsy and exacerbation of brain injury in mice lacking the glutamate transporter GLT-1. *Science* **276**, 1699–1702.
- Tong, G., and Jahr, C.E. (1994). Block of glutamate transporters potentiates postsynaptic excitation. *Neuron* **13**, 1195–1203.
- Trussell, L.O., and Fischbach, G.D. (1989). Glutamate receptor desensitization and its role in synaptic transmission. *Neuron* **3**, 209–218.
- Wadiche, J.I., Arriza, J.L., Amara, S.G., and Kavanaugh, M.P. (1995a). Kinetics of a human glutamate transporter. *Neuron* **14**, 1019–1027.
- Wadiche, J.I., Amara, S.G., and Kavanaugh, M.P. (1995b). Ion fluxes associated with excitatory amino acid transport. *Neuron* **15**, 721–728.
- Wilkin, G.P., Garthwaite, J., and Balazs, R. (1982). Putative acidic amino acid transmitters in the cerebellum. II. Electron microscopic localization of transport sites. *Brain Res.* **244**, 69–80.
- Wyllie, D.J.A., Mathie, A., Symonds, C.J., and Cull-Candy, S.G. (1991). Activation of glutamate receptors and glutamate uptake in identified macroglial cells in rat cerebellar cultures. *J. Physiol.* **432**, 235–258.

Yamamoto, T., Vukelic, J., Hertzberg, E.L., and Nagy, J.I. (1992). Differential anatomical and cellular patterns of connexin43 expression during postnatal development of rat brain. *Dev. Brain Res.* *66*, 165–180.

Zerangue, N., and Kavanaugh, M.P. (1996). Flux coupling in a neuronal glutamate transporter. *Nature* *383*, 634–637.

Zhang, S., and Trussell, L.O. (1994). A characterization of excitatory postsynaptic potentials in the avian nucleus magnocellularis. *J. Neurophysiol.* *72*, 705–718.